Phase reddening effects of pure minerals with different albedo. Yazhou Yang[1,2], R. E. Milliken[2], Hao Zhang[1], and Te Jiang[1]. [1]Planetary Science Institute, China University of Geosciences, Wuhan 430074, China; [2]Dept. Earth, Env., and Planetary Science, Brown University, Providence, RI, 02912, USA. yangyazhou1@gmail.com .

Introduction: Visible-near infrared (VIS-NIR) reflectance spectroscopy is widely used to determine the surface mineralogy of airless bodies. However，interpretation of such spectra can be complicated by changes in spectral slope that are dependent on viewing and scattering geometry [1,2]. For example, with increasing phase angle, the reflectance spectra of many planetary bodies show a reddening trend that is called "phase reddening" [3]. This effect, where reflectance spectra at larger phase angles exhibit a steeper slope, is widely observed on airless asteroids (e.g., Itokawa) [4], and is observable for near-Earth asteroids observed over a wide range in phase angles [5]. Laboratory measurements and simulations have demonstrated that both band depth and reflectance may change with viewing geometry [2,3,6]. As a result, phase reddening caused by phase angle variations could complicate the interpretations of space weathered sample spectra, as reddening is also a well-known effect of space weathering [5].

Schröder et al. [3] and Ruesch et al. [1] have studied the phase reddening effects on terristrial rocks and meteorites, respectively. Here we examine biconcial reflectance measurements of pure minerals with different albedos that are relevant to airless bodies to characterize phase reddening effects as observed with a portable field spectrometer.

Methods: Three minerals with different albedos, labradorite (Lab), olivine (OL), and ilmenite (Ilm), were ground and wet-seived into a size distribution of 63-75 μm. Each sample surface was carefully leveled by moving the edge of a glass slide to obtain a flat surface (Fig. 1). Reflectance measurements were carried out with an ASD FieldSpec3 spectrometer by changing the view zenith angle in the principal plane. All spectra are measred relative to a Spectralon plaque with a nominal reflectance of 99%.

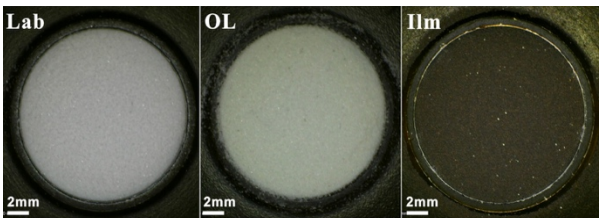

Fig. 1. Images of Lab, OL, and Ilm samples. The particle size is 63-75 μm.

Results: The radiance data of Spectralon measured by the ASD was first divided by the cosine of the emission angle and then scaled to the bidirectional reflectance disturibtion factor data of Spectralon as obtained by the multi-angular imaging spectro-radiometer (MISR) team [7]. As shown in Fig. 2, for a wavelength of 0.63 μm, the ASD measured phase curve agrees well with the MISR data and has a maximum difference less than 1.5%. Absolute reflectance for Spectralon is largely invariant over 0.3~1.7 μm, thus the ASD-measured Spectralon phase curve at 0.633 μm was used to obtain the sample reflectance factor (REFF) defined as:

$$REFF_{sample}(i,e,\lambda) = \frac{DN_{sample}(\mathrm{i,e},\lambda)}{DN_{\mathrm{spectralon}}(\mathrm{i,e},\lambda)} \cdot REFF_{spectralon}(i,e,0.633) \cdot$$

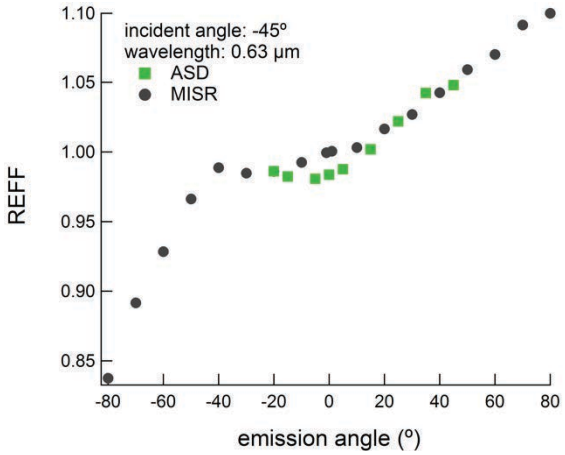

Fig. 2. Comparison of the phase curve of Spectralon obtained by ASD with that of MISR. The ASD data was scaled to MISR data at emission angle of -20°.

All three of the samples measured exhibit a forward scattering component, or enhanced reflectance at larger phase angles. Figure 3 shows the normalized (at 0.55μm) reflectance spectra of Lab, OL and Ilm measured under a fixed incident angle (-45°) and varying viewing zeniths from -20° to 45°. It is seen that the spectral slopes of Lab and OL show phase reddening while that of Ilm exhibits bluing. This difference is also clearly shown in the plot of the 1.5 μm/0.7 μm REFF ratio versus phase angle (Fig. 4).

Fig. 5 shows the normalized (at phase angle 25°) phase curves of Lab, OL and Ilm at wavelengths from 0.4 to 1.5 μm. The phase curves of Lab and OL become steeper at longer wavelength while that of Ilm shows an opposite behavior. The phase curves are much steeper within the aborption bands of OL (~1.0 μm) and Lab (~1.2μm), which have lower reflectance values.

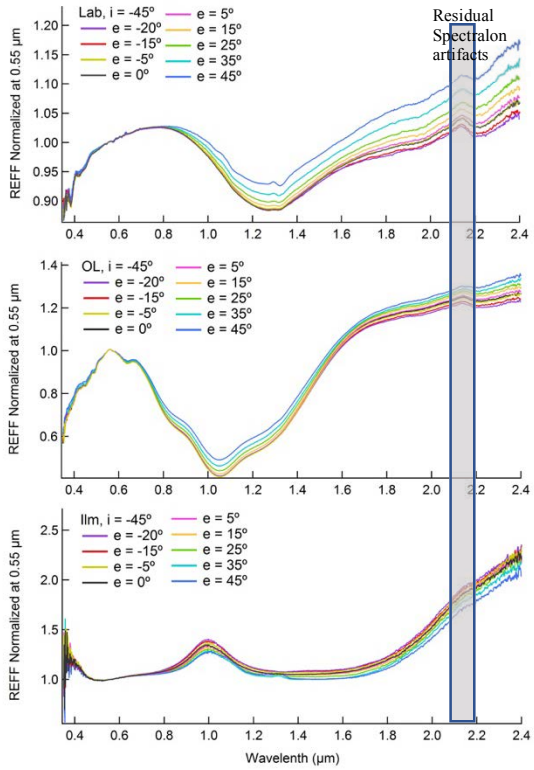

Fig. 3. Normalized reflectance spectra of Lab, OL and Ilm obtained at different viewing angles.

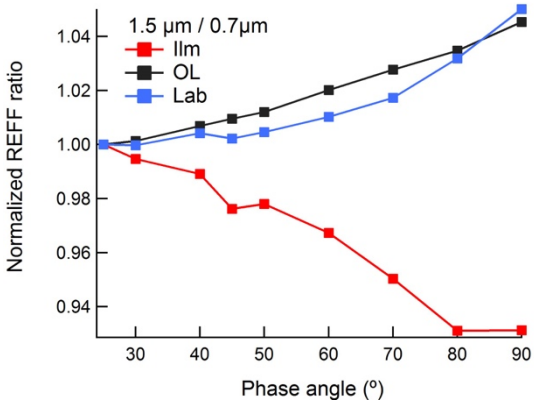

Fig. 4. Normalized color ratio of Lab, OL and Ilm.

Disscussion: The opposite spectral behaviors of the bright samples (Lab and OL) and the dark, opaque Ilm imply the complex nature of phase reddening effects. Complete physical mechanisms for phase reddening are still unclear, but the increased contributions of multiple scattering at large phase angles is a key factor [8]. For dark materials like Ilm, much of the incident radiation is strongly absorbed and that reaching the detector is mainly surface reflections. On the other hand, radiation incident on brighter and more transparent materials like Lab and OL can penetrate deeper in the particulate samples and hence more multiple scattering light can exit the sample.

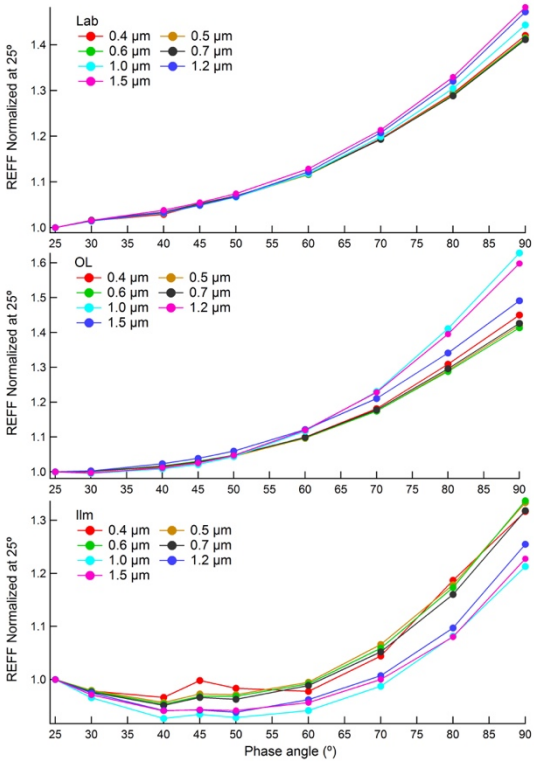

Fig. 5. Normalized phase curves of Lab, OL and Ilm at different wavelengths.

Conclusion: Degree of phase reddening can vary strongly as a function of mineral/sample albedo. Though not unexpected, this highlights the complexity of disentangling phase reddining due to geometry from those of space weathering effects, as the latter can induce darkening (e.g., presence of nanophase Fe) which can in turn affect the geometry-dependent phase reddening of a surface. Use of portable spectrometers such as the FieldSpec is beneficial in that it is rapid, obtains data over a large wavelength range, and can be used in off-axis configurations. Future work consists of quantitatively comparing these results to those obtained by measurements in the NASA RELAB facility and additional measurements for samples with varying particle size, mineral mixtures and packing structures to build upon prevous studies.

References: [1] Ruesch, O., *et al.* (2015) *Icarus*, 258, 384-401. [2] Izawa, M., *et al*. (2016) *Icarus,* 266, 235-248. [3] Schröder, S., *et al*. (2014) *Icarus*, 239, 201-216. [4] Abe M., *et al*. (2006) *Science*, 312, 1334-1338. [5] Sanchez, J., *et al*. (2012) *Icarus*, 220, 36-50. [6] Beck, P., *et al.* (2012) *Icarus*, 218, 364-377. [7] Bruegge, C. *et al*. (2001) *RSE*, 77, 354-366. [8] Hapke, B., *et al.* (2012) *JGR*, 117. [9] Yang Y. et al. (2017) *A&A,* 597, A50.